An Integrated Electromechanical Model of the Fixed-speed Induction Generator for Turbine-Grid Interactions Analysis

Da Xie, *Wangping Wu, Xitian Wang, Chenghong Gu, Yanchi Zhang, Furong Li*

Abstract — When wind turbine is connected to the power grid, the turbine-grid interactions restrict its lifespan and produce adverse effects to the grid. Electrical or mechanical oscillations caused by turbine-grid interactions could gradually be weakened or amplified seriously at a certain frequency. This paper discusses all types of interactions between a wind turbine and the grid and the influence of the initial operating point, the parallel capacitor and the series capacitor on the stability of system. Firstly, an integrated dynamic electromechanical model of a single fixed-speed induction generator (FSIG) wind generation system is derived based on the small signal model of each element. Then, a method of stability analysis based on Kharitonov theorem is introduced. Then, the model details the frequency and damping ratio of oscillation mode and classifies those modes' interactions according to participation factors, followed by time domain simulations by the single FSIG generation system to testify the results. Finally, the paper studies all the oscillation modes when the initial operating point, the parallel capacitor or the series capacitor change in the integrated model, which can be verified by Kharitonov polynomials. The indicative findings help to design the damping control to mitigate turbine-grid interactions.

Index terms— Fixed-speed induction generator (FSIG), Electrical resonance, Sub-synchronous interaction (SSI), Low-frequency oscillation, Kharitonov polynomials

1. INTRODUCTION

Policies supporting renewable energy development adopted by several countries have encouraged significant investments in wind power [1]. As a result, wind power capacity in North America and Europe has grown at a rate of 20% to 40% per year over the past decade [2]. However, there are some operation problems in interactions between wind turbines and the grid, such as growing SSI incidents with other power system components [3], low-frequency oscillation in the transmission line [4], excessive stress and fatigue on the gearbox [5], un-expected tripping-off of large-scale wind farms from the grid [6], and et al.[7]. These problems have shortened the life of wind turbines, adding to the total cost of large-scale wind energy development. They have also caused significant power quality problems like harmonic, flicker and power factor problems in the power system.

Several types of oscillations occur frequently, such as electrical resonance, SSI including sub-synchronous resonance (SSR) and sub-synchronous oscillation (SSO) and low-frequency oscillation[8]. Electrical resonance will occur and DFIGs provide energy for this resonance continuously, if there is system equivalent inductance $x \approx 0$ at certain sub-synchronous frequency[9].SSR is a condition where the wind farm exchanges energy with the power grid at one or more natural frequencies of the electrical or mechanical part of the power system[10]. Frequency of this energy exchange is below the fundamental frequency of the system, and this may result in shaft failure[11]. There is a risk of sub-synchronous control interaction (SSCI) even if the level of compensation is very low, such as less than 10%. However, the probability of occurrence of sub-synchronous resonance (SSR) is greatly reduced [12, 13]. SSO and harmonic resonance can occur between WFs and HVDC(High Voltage Direct Current) systems [14]. The oscillations can appear in the presence of background harmonics and is arguably resulting from the controller interaction of the wind energy conversion system (WECS) converter controller and HVDC converter controller [15]. Low-frequency oscillations occur when the rotors of machines, behaving as rigid bodies, oscillate with respect to each other using the electrical transmission path between them for exchanging energy [16]. In the conventional boost converter with pulse train (PT) control, the output voltage will produce undesirable low frequency oscillation in continuous conduction mode[16].

Improper electrical parameter settings might also influence dynamic characteristics of the whole wind generation system [17]. Reference [18] designs a robust controller under uncertain operating conditions by Kharitonov theorem.

Reference [19] deals with proposal of new method based on Kharitonov theorem to find feasible parameters. A robust PID control design for uncertain system through Kharitonov theorem has been reported in [20].

Even though there is a sufficient understanding of the interactions between wind turbines and the grid, the problem that most of the related researches only focus on the part of the interactions still exists. A detailed linear state space model is presented for the wind farm and the transmission system in [21] to present the potential of sub-synchronous resonance in large wind farms based on double-cage induction generators connected to a series-compensated line. The torsional dynamics of a doubly fed induction generator (DFIG)-based wind turbines is investigated, as in [22]. Both active power and reactive power modulation controls are developed. The stator dynamics of induction generators is included in [23] to quantify the low-frequency oscillation characteristics of wind power systems. A small signal stability analysis is performed in [24] to analyze torsional oscillation phenomenon of a wind turbine with DFIG, which is an accurate method in calculating torsional oscillation frequency of a wind turbine. Reference [8] presents a frequency scan to determine the SSI frequency and a detailed small signal analysis to study participated factors.

Another problem is that there are very few researchers studying the interactions between Fixed-speed induction generator (FSIG) and the grid. Although FSIG has been replaced, many FSIGs used in some wind farm are still operating in many countries. The electrical and mechanical oscillations of FSIG wind farms are also a common and serious problem to which farm owners and grid corporations pay much attention.

In this paper, all electrical and mechanical oscillations are collectively named as turbine-grid interactions. An integrated electromechanical model of a single FSIG generation system is derived to observe all oscillation modes' details and determine each oscillation's category of interactions according to participation factors. The results are justified by time domain simulations. This paper also investigates the turbine-grid interactions when the initial operating point, the parallel capacitor or the series capacitor changes, which are verified through the analysis of Kharitonov polynomials.

The main contributions of this paper are that: 1) the proposed model can find all oscillation modes between a wind turbine and the grid and determines every mode's category; 2) it conducts a more comprehensive and effective study on the dynamic stability of a single FSIG system; 3) it studies the influence of the initial operating point, the parallel capacitor and the series capacitor on the oscillation frequencies and the damping ratios of all the oscillation modes; 4) the appropriate range of values of initial operating point, series capacitor compensation and parallel capacitor compensation in the system can be obtained by eigenvalue analysis method or using Kharitonov's polynomials.

The other sections of this paper are organized as follows. In section II, the small signal model of FSIG generation system is presented. Section III introduces a method of stability analysis based on Kharitonov theorem. Section IV uses time domain simulations to confirm the preliminary work of Section II. Section V also studies the influence the initial operating point, the parallel capacitor and the series capacitor may have on turbine-grid interactions, which are verified by the method mentioned above. Section VI concludes the paper.

2. ELECTROMECHANICAL MODEL OF A SINGLE FSIG WIND GENERATION SYSTEM

A single FSIG wind generation system in Fig.1 is composed of a mechanical system and an electrical system. The mechanical model (including the blade, gearbox, low-speed shaft, high-speed shaft and generator rotor) is made up of three masses. The induction generator (IG), parallel compensation capacitor, transformer, transmission line and the series compensation capacitor of the electrical system are then modeled respectively. Detailed parts of those models are presented as follows.

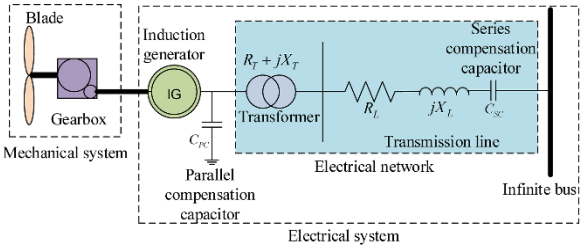

Fig. 1 Diagram of a single FSIG wind generation system

2.1. Mechanical system model

Similar to the steam turbine, the mechanical system of a FSIG is modeled by an equivalent multi-mass system. Based on the state equation of the three-mass system in [25] and a set of properly selected base values, a per-unit small signal model for mechanical system is developed.

$$\begin{cases} \Delta \dfrac{\mathrm{d}}{\mathrm{d}t}\mathbf{X}_M = \mathbf{A}_M \Delta \mathbf{X}_M + \mathbf{B}_M \Delta \mathbf{u}_M \\ \Delta \mathbf{Y}_M = \mathbf{C}_M \Delta \mathbf{X}_M + \mathbf{D}_M \Delta \mathbf{u}_M \end{cases} \tag{1}$$

Subscript *M* denotes the three-mass shaft model, "Δ" denotes a small deviation.

$$\Delta \mathbf{X}_M = \begin{bmatrix} \Delta\theta_1 & \Delta\theta_2 & \Delta\theta_3 & \Delta\omega_1 & \Delta\omega_2 & \Delta\omega_3 \end{bmatrix}^T \quad ; \quad \Delta \mathbf{Y}_M = \begin{bmatrix} \Delta\theta_3 & \Delta\omega_3 \end{bmatrix}^T \quad ; \quad \Delta \mathbf{u}_M = \begin{bmatrix} \Delta T_w & \Delta T_e \end{bmatrix}^T \quad ;$$

$$\mathbf{A}_M = \begin{bmatrix} 0 & 0 & 0 & \omega_b & 0 & 0 \\ 0 & 0 & 0 & 0 & \omega_b & 0 \\ 0 & 0 & 0 & 0 & 0 & \omega_b \\ -\dfrac{K_{12}}{2H_1} & \dfrac{K_{12}}{2H_1} & 0 & -\dfrac{D_1+D_{12}}{2H_1} & \dfrac{D_{12}}{2H_1} & 0 \\ \dfrac{K_{12}}{2H_2} & -\dfrac{K_{12}+K_{23}}{2H_2} & \dfrac{K_{23}}{2H_2} & \dfrac{D_{12}}{2H_2} & -\dfrac{D_2+D_{12}+D_{23}}{2H_2} & \dfrac{D_{23}}{2H_2} \\ 0 & \dfrac{K_{23}}{2H_3} & -\dfrac{K_{23}}{2H_3} & 0 & \dfrac{D_{23}}{2H_3} & -\dfrac{D_3+D_{23}}{2H_3} \end{bmatrix}; \quad \mathbf{B}_M = \begin{bmatrix} 0 & 0 \\ 0 & 0 \\ 0 & 0 \\ \dfrac{1}{2H_1} & 0 \\ 0 & 0 \\ 0 & -\dfrac{1}{2H_3} \end{bmatrix};$$

$$\mathbf{C}_M = \begin{bmatrix} 0 & 0 & 1 & 0 & 0 & 0 \\ 0 & 0 & 0 & 0 & 0 & 1 \end{bmatrix}; \mathbf{D}_M = \mathbf{0}_{2\times 2}.$$

where, θ_i and ω_i (i=1,2,3) are the mechanical rotation angle and the angular velocity of mass i, T_w is the wind torque of mass 1 and T_e is the electromagnetic torque of mass 3, H, D and K denote the moment of inertia, the damping coefficient and the elastic coefficient of the three masses respectively.

2.2. Electrical system model

2.2.1. Induction generator

The five-order model of the induction generator (IG) is adopted in [21]. Then the standard state equation of the per-unit small signal model of IG can be expressed as:

$$\begin{cases} \Delta \dfrac{\mathrm{d}}{\mathrm{d}t}\mathbf{X}_{IG} = \mathbf{A}_{IG} \Delta \mathbf{X}_{IG} + \mathbf{B}_{IG} \Delta \mathbf{u}_{IG} \\ \Delta \mathbf{Y}_{IG} = \mathbf{C}_{IG} \Delta \mathbf{X}_{IG} + \mathbf{D}_{IG} \Delta \mathbf{u}_{IG} \end{cases} \tag{2}$$

Subscript *IG* denotes induction generator, and

$$\Delta \mathbf{X}_{IG} = \begin{bmatrix} \Delta\psi_{qs} & \Delta\psi_{ds} & \Delta\psi_{qr} & \Delta\psi_{dr} \end{bmatrix}^T ; \Delta \mathbf{Y}_{IG} = \begin{bmatrix} \Delta i_{qs} & \Delta i_{ds} & \Delta T_e \end{bmatrix}^T ; \Delta \mathbf{u}_{IG} = \begin{bmatrix} \Delta u_{qs} & \Delta u_{ds} & \Delta u_{qr} & \Delta u_{dr} & \Delta\omega_r \end{bmatrix}^T ;$$

$$\mathbf{A}_{IG}=\begin{bmatrix} -\frac{\omega_b R_s X_{rr}}{L} & -\omega_s\omega_b & \frac{\omega_b R_s X_m}{L} & 0 \\ \omega_s\omega_b & -\frac{\omega_b R_s X_{rr}}{L} & 0 & \frac{\omega_b R_s X_m}{L} \\ \frac{\omega_b R_r X_m}{L} & 0 & -\frac{\omega_b R_r X_{ss}}{L} & -s_{r0}\omega_s\omega_b \\ 0 & \frac{\omega_b R_r X_m}{L} & s_{r0}\omega_s\omega_b & -\frac{\omega_b R_r X_{ss}}{L} \end{bmatrix};\ \mathbf{B}_{IG}=\begin{bmatrix} \omega_b & 0 & 0 & 0 & 0 \\ 0 & \omega_b & 0 & 0 & 0 \\ 0 & 0 & \omega_b & 0 & \omega_s\omega_b\psi_{dr0} \\ 0 & 0 & 0 & \omega_b & -\omega_s\omega_b\psi_{qr0} \end{bmatrix};$$

$$\mathbf{C}_{IG}=\begin{bmatrix} \frac{X_{rr}}{L} & 0 & -\frac{X_m}{L} & 0 \\ 0 & \frac{X_{rr}}{L} & 0 & -\frac{X_m}{L} \\ \frac{X_m}{L}\psi_{dr0} & -\frac{X_m}{L}\psi_{qr0} & -\frac{X_m}{L}\psi_{ds0} & \frac{X_m}{L}\psi_{qs0} \end{bmatrix};\ \mathbf{D}_{IG}=\mathbf{0}_{3\times5}\circ$$

where, Ψ,i and u denote the flux, the current and the voltage of IG, whose subscript s and r denote the stator and the rotor respectively, and subscript d, q denote the components in d-q frame, $\Delta\omega_r$ is the angular velocity of the generator rotor, subscript '0' denotes the steady-state value of the initial operating point, s_0 is the slip of IG, R_s and R_r are the resistance of the stator windings and the rotor windings, ω_s is the synchronous angular velocity, ω_b is the base angular velocity, X_s and X_r are the reactance of the stator windings and the rotor windings, X_m is the excitation reactance.$L=X_sX_r+(X_s+X_r)X_m$, $X_{ss}=X_s+X_m$, $X_{rr}=X_r+X_m$.

2.2.2. Electrical network and parallel compensation capacitor

Electrical network consists of a transformer and a transmission line (including the series compensation capacitor). The network is modeled as a RLC part, as shown in [26]. The RLC model is established in *x-y* reference frame in order to be connected to the mechanical system model. The equations for the per-unit small signal model of RLC model are

$$\begin{cases} \Delta\frac{\mathrm{d}}{\mathrm{d}t}\mathbf{X}_{RLC}=\mathbf{A}_{RLC}\Delta\mathbf{X}_{RLC}+\mathbf{B}_{RLC}\Delta\mathbf{u}_{RLC} \\ \Delta\mathbf{Y}_{RLC}=\mathbf{C}_{RLC}\Delta\mathbf{X}_{RLC}+\mathbf{D}_{RLC}\Delta\mathbf{u}_{RLC} \end{cases} \tag{3}$$

where

$$\Delta\mathbf{X}_{RLC}=\begin{bmatrix}\Delta i_{L,x} & \Delta i_{L,y} & \Delta u_{SC,x} & \Delta u_{SC,y}\end{bmatrix}^T;\ \Delta\mathbf{Y}_{RLC}=\begin{bmatrix}\Delta i_{L,x} & \Delta i_{L,y}\end{bmatrix}^T;\ \Delta\mathbf{u}_{RLC}=\begin{bmatrix}\Delta u_{x1} & \Delta u_{y1} & \Delta u_{x2} & \Delta u_{y2}\end{bmatrix}^T;$$

$$\mathbf{A}_{RLC}=\begin{bmatrix} -\frac{\omega_b r}{x} & \omega_b & -\omega_b/x & 0 \\ -\omega_b & -\frac{\omega_b r}{x} & 0 & -\frac{\omega_b}{x} \\ -\omega_b x_c & 0 & 0 & \omega_b \\ 0 & -\omega_b x_c & -\omega_b & 0 \end{bmatrix};\ \mathbf{B}_{RLC}=\begin{bmatrix} \frac{\omega_b}{x} & 0 & -\frac{\omega_b}{x} & 0 \\ 0 & \frac{\omega_b}{x} & 0 & -\frac{\omega_b}{x} \\ 0 & 0 & 0 & 0 \\ 0 & 0 & 0 & 0 \end{bmatrix};\ \mathbf{C}_{RLC}=\begin{bmatrix} 1 & 0 & 0 & 0 \\ 0 & 1 & 0 & 0 \end{bmatrix};\ \mathbf{D}_{RLC}=\mathbf{0}_{2\times2}.$$

i_L and u_{SC} denote the current of the inductor and the voltage of the series compensation capacitor respectively, $r=r_T+r_L$, r_T is the resistance of the transformer and r_L is the resistance of the transmission line; $x=x_T+x_L+x_{SC}$, x_T is the reactance of the transformer, x_L is the reactance of the transmission line and x_{SC} is the reactance of the series compensation capacitor.

The per-unit model of the parallel compensation capacitor is similar to the per-unit model of the electrical network. And it is easier to be obtained after removing the resistor and inductor in (3).

2.3. Integrated electromechanical model

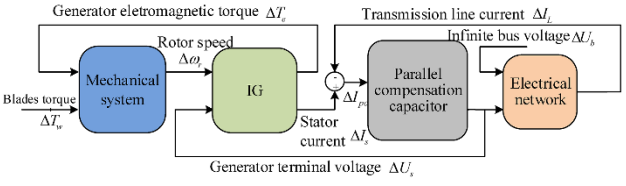

Fig. 2 Integrated electromechanical model of a single FSIG wind generation system

The integrated electromechanical model of a single FSIG wind generation system based on the equations above is given as follows:

$$\begin{cases} \Delta\dfrac{\mathrm{d}}{\mathrm{d}t}\mathbf{X}_{FSIG} = \mathbf{A}_{FSIG}\Delta\mathbf{X}_{FSIG} + \mathbf{B}_{FSIG}\Delta\mathbf{u}_{FSIG} \\ \Delta\mathbf{Y}_{FSIG} = \mathbf{C}_{FSIG}\Delta\mathbf{X}_{FSIG} + \mathbf{D}_{FSIG}\Delta\mathbf{u}_{FSIG} \end{cases} \tag{4}$$

where subscript *FSIG* denotes the FSIG wind generation system and subscript *PC* denotes the parallel compensation capacitor.

$$\Delta\mathbf{X}_{FSIG} = \begin{bmatrix} \Delta\mathbf{X}_M & \Delta\mathbf{X}_{IG} & \Delta\mathbf{X}_{PC} & \Delta\mathbf{X}_{RLC} \end{bmatrix}^T;\ \Delta\mathbf{Y}_{FSIG} = \begin{bmatrix} \Delta i_x & \Delta i_y \end{bmatrix}^T;\ \Delta\mathbf{u}_{FSIG} = \begin{bmatrix} \Delta T_w \end{bmatrix};$$

$$\mathbf{A}_{FSIG} = \begin{bmatrix} \mathbf{A}_M & \mathbf{A}_{G-M} & & \\ \mathbf{A}_{M-G} & \mathbf{A}_G & \mathbf{A}_{PC-G} & \\ & \mathbf{A}_{G-PC} & \mathbf{A}_{PC} & \mathbf{A}_{RLC-PC} \\ & & \mathbf{A}_{PC-RLC} & \mathbf{A}_{RLC} \end{bmatrix};\ \mathbf{B}_{FSIG} = \begin{bmatrix} 0 & 0 & 0 & \dfrac{1}{2H_1} & 0 & 0 & 0 & 0 & 0 & 0 & 0 & 0 & 0 \end{bmatrix}^T;$$

$$\mathbf{C}_{FSIG} = \begin{bmatrix} 0 & 0 & 0 & 0 & 0 & 0 & 0 & 0 & 0 & 0 & 0 & 0 & 1 & 0 \\ 0 & 0 & 0 & 0 & 0 & 0 & 0 & 0 & 0 & 0 & 0 & 0 & 0 & 1 \end{bmatrix};\ \mathbf{D}_{FSIG} = \mathbf{0}_{14\times 1}\circ$$

3. THE STABILITY ANALYSIS METHOD BASED ON KHARITONOV THEOREM

In engineering practice, the model parameters of the system often have some uncertainty. For the single FSIG system shown by Fig.1, the series capacitor compensation and the parallel capacitor compensation are reset more often than other parameters, and the initial steady-state operating point may also change. However, parametric variation may have an adverse impact on the stability and dynamic performance of the system. Hence, it is necessary to analyze the stability of the system, whose parameters change in a given range. It is an effective way to solve the problem by applying the interval model in engineering practice when the model parameter is difficult to describe with precise mathematical relation.

Consider the interval polynomial of the system as

$$K(s) = \sum_{i=0}^{n} a_i s^i \qquad a_i \in [a_{il}, a_{iu}] \tag{5}$$

where, a_{il} and a_{iu} ($i=1,2,3,\cdots,n$) represent the lower limit and the upper limit of a_i respectively.

For the interval system described above, it is not easy to determine the stability simply through calculating the eigenvalue or applying Routh Hurwitz stability criterion. The Kharitonov theorem is effective in the stability analysis of the interval system, and it is convenient and quick to determine the stability of the interval polynomial.

According to the Kharitonov theorem, an interval polynomial set with invariant degree is stable if and only if it's four Kharitonov polynomials are stable, which are consisted of two distinct even and odd parts, and can be represented as

$$\begin{cases} K_1(s) = K_{\min}^{even} + K_{\min}^{odd} \\ K_2(s) = K_{\min}^{even} + K_{\max}^{odd} \\ K_3(s) = K_{\max}^{even} + K_{\min}^{odd} \\ K_4(s) = K_{\max}^{even} + K_{\max}^{odd} \end{cases} \tag{6}$$

where,

$$\begin{cases} K_{\min}^{even} = a_{0l} + a_{2u}s^2 + a_{4l}s^4 + a_{6u}s^6 \cdots \\ K_{\max}^{even} = a_{0u} + a_{2l}s^2 + a_{4u}s^4 + a_{6l}s^6 \cdots \\ K_{\min}^{odd} = a_{1l}s + a_{3u}s^3 + a_{5l}s^5 + a_{7u}s^7 \cdots \\ K_{\max}^{odd} = a_{1u}s + a_{3l}s^3 + a_{5u}s^5 + a_{7l}s^7 \cdots \end{cases} \tag{7}$$

That is

$$\begin{cases} K_1(s) = a_{0l} + a_{1l}s + a_{2u}s^2 + a_{3u}s^3 + a_{4l}s^4 + \ldots \\ K_2(s) = a_{0l} + a_{1u}s + a_{2u}s^2 + a_{3l}s^3 + a_{4l}s^4 + \ldots \\ K_3(s) = a_{0u} + a_{1l}s + a_{2l}s^2 + a_{3u}s^3 + a_{4u}s^4 + \ldots \\ K_4(s) = a_{0u} + a_{1u}s + a_{2l}s^2 + a_{3l}s^3 + a_{4u}s^4 + \ldots \end{cases} \tag{8}$$

Meanwhile, the stability of Kharitonov polynomials can be determined by applying Hurwitz criterion for the constant parameters of the system.

4. ANALYSIS AND SIMULATION RESULTS

According to the parameters shown in the appendix, the integrated electromechanical model of a single FSIG wind generation system is established in Matlab/Simulink, and whose results are presented.

4.1. Initialization of the model

The mathematical model needs the initial steady-state operating point of the system to initialize itself. When the system is steady, time derivatives of all state variables is zero, namely $dx_0/dt=0$. Based on the parameters in the appendix, the initial operating point is obtained as follows.

TABLE 1

INITIAL OPERATING POINT OF A SINGLE FSIG WIND GENERATION SYSTEM

Active power	reactive power	Rotor slip	Generator voltage
0.9000 p.u.	-0.4216 p.u.	-0.0054	1 p.u.

4.2. Analysis results of the model

The rated power of a FSIG is 2MW and the generator voltage is 0.69kV. The eigenvalues of state matrix $\mathbf{A}_{FSIG}$ of the system are listed in Table 2.

TABLE 2

EIGENVALUES OF AFSIG OF A SINGLE FSIG WIND GENERATION SYSTEM

Mode	Eigenvalue	Frequency/Hz	Damping ratio
1	-7.355±1,348.182i	214.570	0.0055
2	-10.192±720.212i	114.625	0.0142
3	-15.522±509.453i	81.082	0.0305
4	-15.362±118.741i	18.898	0.1283
5	-0.144±78.071i	12.425	0.0018
6	-1.038±10.831i	1.724	0.0954
7	-1.012±3.114i	0.496	0.3092

In Table 2, there exist seven oscillation modes in a single FSIG system, describing all the interactions between the wind turbine and the grid. To determine each mode's category of interactions, participation factor is used as a measure of the association between the state variables and the modes. The system state variables ΔX_{FSIG} is detailed as

$$\begin{aligned} \Delta\mathbf{X}_{FSIG} = \big[&\Delta\theta_1 \quad \Delta\theta_2 \quad \Delta\theta_3 \quad \Delta\omega_1 \quad \Delta\omega_2 \quad \Delta\omega_3 \\ &\Delta\psi_{qs} \quad \Delta\psi_{ds} \quad \Delta\psi_{qr} \quad \Delta\psi_{dr} \quad \Delta u_{PC,x} \\ &\Delta u_{PC,y} \quad \Delta i_{L,x} \quad \Delta i_{L,y} \quad \Delta u_{SC,x} \quad \Delta u_{SC,y}\big]^T \end{aligned} \tag{9}$$

u_{PC} denotes the voltage of parallel compensation capacitor. The participation factors of state variables to the oscillation modes are shown in Table 3.

TABLE 3

PARTICIPATION FACTORS OF STATE VARIABLES TO OSCILLATION MODES

	Mode1	Mode2	Mode3	Mode4	Mode5	Mode6	Mode7
$\Delta\ \theta_1$	0.0000	0.0000	0.0000	0.0000	0.0002	0.0858	**0.3551**
$\Delta\ \theta_2$	0.0000	0.0000	0.0000	0.0000	**0.4453**	0.0419	0.0044
$\Delta\ \theta_3$	0.0000	0.0000	0.0000	0.0001	0.0546	**0.3845**	**0.2305**
$\Delta\ \omega_1$	0.0000	0.0000	0.0000	0.0000	0.0002	0.0858	**0.3552**
$\Delta\ \omega_2$	0.0000	0.0000	0.0000	0.0000	**0.4453**	0.0420	0.0045
$\Delta\ \omega_3$	0.0001	0.0007	0.0000	0.0007	0.0545	**0.3646**	0.0241
$\Delta\ \Psi_{qs}$	**0.2440**	**0.2442**	0.0059	0.0058	0.0000	0.0014	0.0008
$\Delta\ \Psi_{ds}$	**0.2442**	**0.2435**	0.0058	0.0054	0.0002	0.0019	0.0008
$\Delta\ \Psi_{qr}$	0.0012	0.0043	0.0000	0.0005	0.0003	**0.1360**	**0.2784**
$\Delta\ \Psi_{dr}$	0.0012	0.0041	0.0000	0.0010	0.0002	**0.1297**	**0.3503**
$\Delta u_{PC,x}$	**0.2498**	**0.2491**	0.0002	0.0002	0.0001	0.0027	0.0012
$\Delta u_{PC,y}$	**0.2496**	**0.2498**	0.0002	0.0002	0.0000	0.0026	0.0016
$\Delta i_{L,x}$	0.0058	0.0058	**0.2450**	**0.2459**	0.0001	0.0016	0.0012
$\Delta i_{L,y}$	0.0058	0.0059	**0.2449**	**0.2454**	0.0001	0.0023	0.0007
$\Delta u_{SC,x}$	0.0002	0.0002	**0.2506**	**0.2509**	0.0001	0.0009	0.0003
$\Delta u_{SC,y}$	0.0002	0.0002	**0.2506**	**0.2511**	0.0001	0.0007	0.0005

In Table 3, bold participation factors mean that the corresponding system state variables play a leading role in those oscillation modes. On the basis of the association between the state variables and the oscillation modes shown by participation factors, each mode's category of interactions can be determined. Classification of the turbine-grid interactions in a FSIG-based generation system is shown in fig. 3.

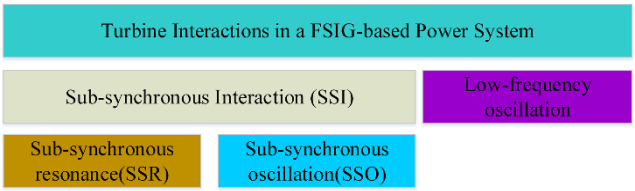

Fig. 3 Classification of turbine-grid interactions in a FSIG-based generation system

4.2.1. Electrical resonance

A passive electric circuit containing an inductor or an iron core coil and a capacitor behaves as a pure resistor element circuit at a power supply of a particular frequency. Active power oscillation caused by harmonics of resonance frequency attenuates slowly when electrical resonance happens. Mode 1 (214.570Hz) is caused by electrical resonance of generator stator reactance and parallel compensation capacitor because $\Delta\ \Psi_{qs}$, $\Delta\ \Psi_{ds}$ and $\Delta u_{PC,x}$, $\Delta u_{PC,y}$ have major relative participation in the mode. The participation factors are 0.2440 for $\Delta\ \Psi_{qs}$, 0.2442 for $\Delta\ \Psi_{ds}$, 0.2498 for $\Delta u_{PC,x}$ and 0.2496 for $\Delta u_{PC,y}$. Mode 2 (114.625Hz) is also electrical resonance mode because those state variables playing major role are the same. The participation factors are 0.2442 for $\Delta\ \Psi_{qs}$, 0.2435 for $\Delta\ \Psi_{ds}$, 0.2491 for $\Delta u_{PC,x}$ and 0.2498 for $\Delta u_{PC,y}$.

4.2.2. Sub-synchronous interaction

SSI is a terminology in power system that describes the energy exchange phenomenon between two power parts at one or more natural frequencies below the synchronous frequency. It happens in the combined wind generation system, which can be divided into sub-synchronous resonance (SSR) and sub-synchronous oscillation (SSO).

①Sub-synchronous resonance

SSR comes from the self-excitation current in the generator stator of a frequency below the synchronous

frequency. The self-excitation current brings about rotating magnetic field of the same frequency. When series capacitor compensation is used in the transmission line, the self-excitation current could arise easily. Small disturbances in the line excite stator currents at frequencies $\pm f_e$, producing a stator flux at same frequencies. As a result, currents in the rotor winding will be induced at the complementary frequency $f_s \pm f_e$.

In Mode 3 (81.082Hz) and Mode 4 (18.898Hz), $\Delta i_{L,x}$, $\Delta i_{L,y}$ and $\Delta u_{SC,x}$, $\Delta u_{SC,y}$ play a major role whereas $\Delta \Psi_{qs}$, $\Delta \Psi_{ds}$ play a secondary role. Based on the line parameters and (4), the electric resonance of transmission line is f_e =31.6Hz, SSR frequency is $f_s \pm f_e$ (81.6Hz or 18.4Hz), in accordance with the two modes. As a result, Mode 3 and Mode 4 belong to sub-synchronous resonance, the resonance frequencies change with the series compensation degree k_{com}.

②Sub-synchronous oscillation

SSO behaves as torsional oscillation of generator shaft near the natural frequency of main components, which arises because some improper settings of electrical parameter might influence dynamic characteristics of mechanical systems or even result in oscillation.

Mode 5 (12.425Hz) is subject to the sub-synchronous oscillation of low-speed shaft because $\Delta \theta_2$ and $\Delta \omega_2$ play the leading participation. The participation factors are both 0.4453 for $\Delta \theta_2$ and $\Delta \omega_2$. Mode 6 (1.724Hz) is subject to the sub-synchronous oscillation of high-speed shaft because $\Delta\theta_3$ and $\Delta \omega_3$ play the leading participation when $\Delta \Psi_{qr}$ and $\Delta \Psi_{dr}$ play the minor one. The participation factors are 0.3845 for $\Delta \theta_3$, 0.3646 for $\Delta \omega_2$, 0.1360 for $\Delta \Psi_{qr}$ and 0.1297 for $\Delta \Psi_{dr}$.

4.2.3. Low-frequency oscillation

Low-frequency oscillation behaves as un-damped oscillation or increasing oscillation of mechanical rotation angle and angular velocity of generator rotator or some other electrical variables involved, whose frequencies normally fall in the range of 0.1Hz and 2.5Hz. Mode 7 (0.496Hz) is caused by low-frequency oscillation of generator rotator because $\Delta \theta_1$, $\Delta \theta_3$, $\Delta\omega_1$, $\Delta \Psi_{qr}$ and $\Delta \Psi_{dr}$ have major relative participation in the mode. The oscillation frequency is slow enough, too. The participation factors are 0.3551 for $\Delta \theta_1$, 0.2305 for $\Delta \theta_3$, 0.3552 for $\Delta \omega_1$, 0.2784 for $\Delta \Psi_{qr}$ and 0.3503 for $\Delta \Psi_{dr}$.

4.3. Time domain simulations

Time domain simulations are used to confirm the indicative findings of the mathematical model. Based on the same parameters of the wind generation system, time domain model is set up in MATLAB/Simulink. The model makes a small disturbance such as a small drop of bus voltage amplitude, a small drop of the wind torque T_w or some other types of disturbance. The simulation results are shown in Fig.4.

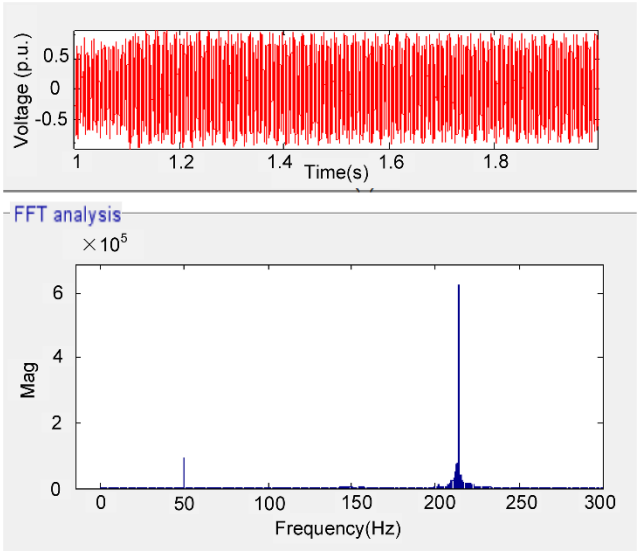

(a) Parallel compensation capacitor voltage and the FFT results (214.570Hz)

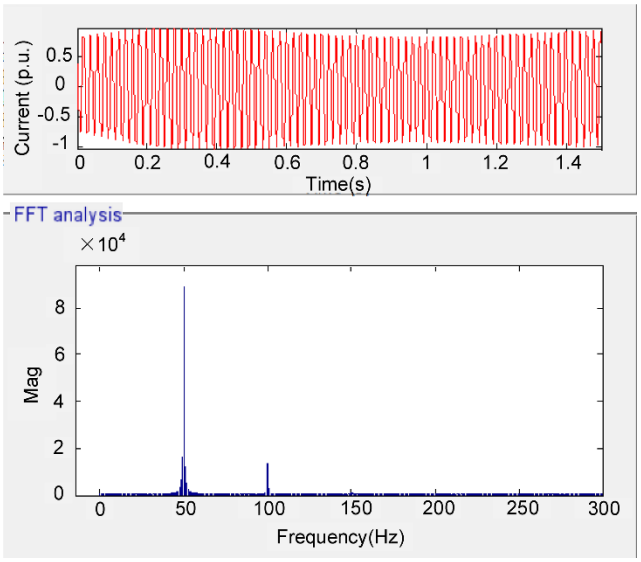

(b) Parallel compensation capacitor current and the FFT results(114.625Hz)

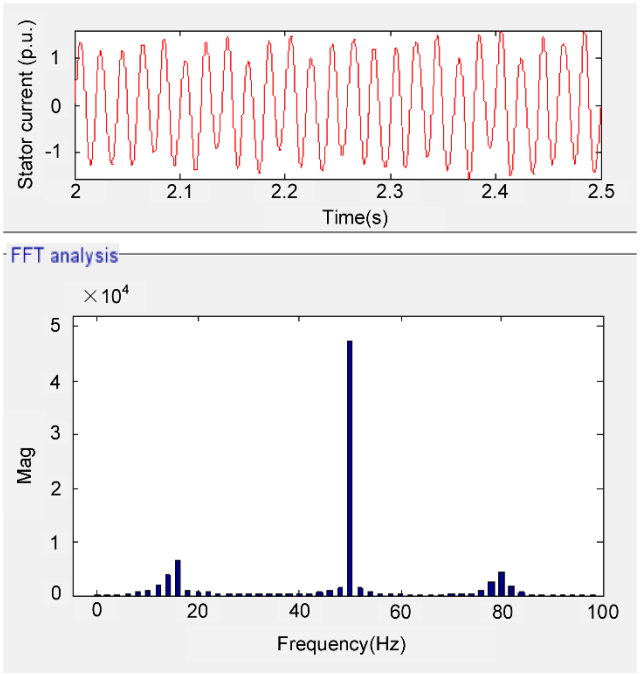

(c) Stator output current and the FFT results (81.082Hz and 18.898Hz)

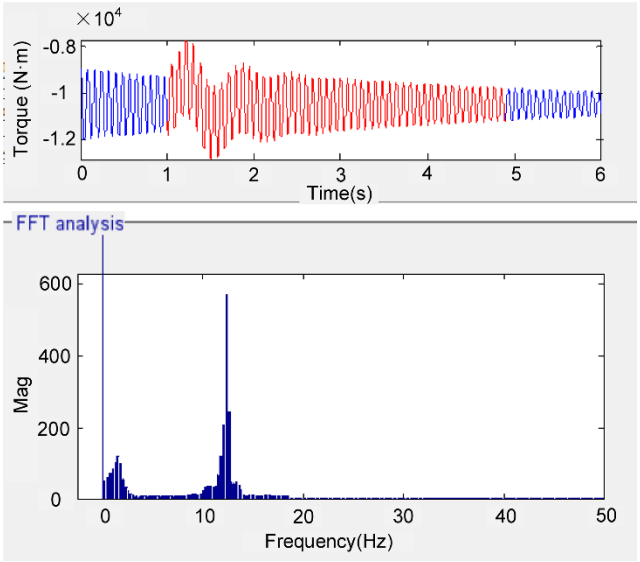

(d) Generator torque and the FFT results (12.425Hz and 1.724Hz)

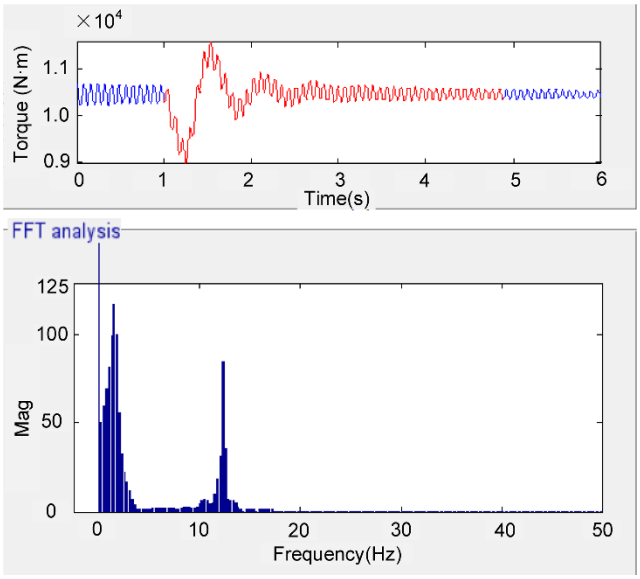

(e) Low speed shaft torque and the FFT results (12.425Hz and 1.724Hz)

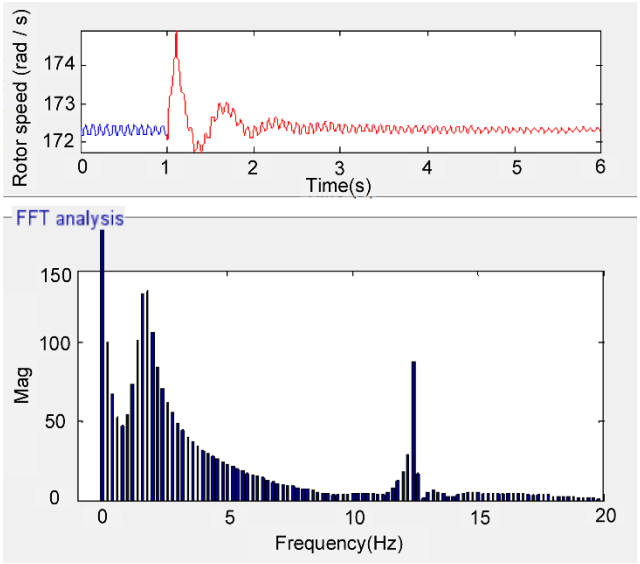

(f) Generator rotation speed and) the FFT results (0.496Hz)

Fig. 4 Time domain simulation results of turbine-grid interactions

5. INFLUENCING FACTORS OF TURBINE-GRID INTERACTIONS

Turbine-grid interactions in a single FSIG system shown by Fig.1 can be influenced by resetting the system's parameters to change its dynamic stability and oscillation frequency. This section discusses the FSIG system's dynamic stability (revealed by eigenvalues of A_{FSIG}) when the initial operating point, the parallel capacitor or the series capacitor change in the first three parts, separately. Then, the proposed method based on Kharitonov polynomials is used to analyze the stability of the established system with variable parameters in the fourth part to verify the rationality of the previous three parts.

5.1. Initial operating point

Table 1 shows the initial steady-state operating point of FSIG system based on the supposition that the active power output of generator is 0.9 p.u., denoted by *Gen.Pe*. Some of the rules are concluded when *Gen.Pe* changes from 0.1 to 1 by a step of 0.01 when other parameters remain the same. Variation trend of the oscillation modes for turbine-grid interactions with *Gen.Pe* is obtained in Fig. 5. The vertical axis represents *Gen.Pe*. The horizontal axis shows frequency or damping ratio, and '*' means stable whereas 'º' means unstable.

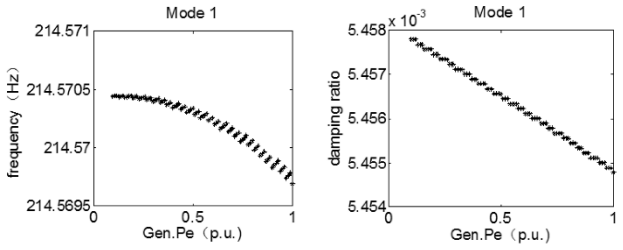

(a) Mode 1

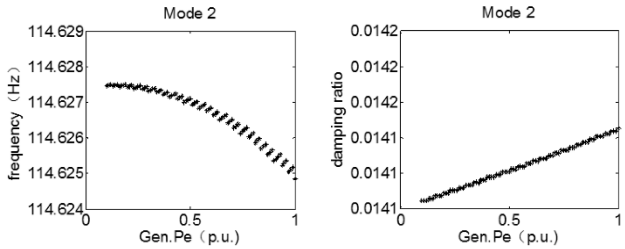

(b) Mode 2

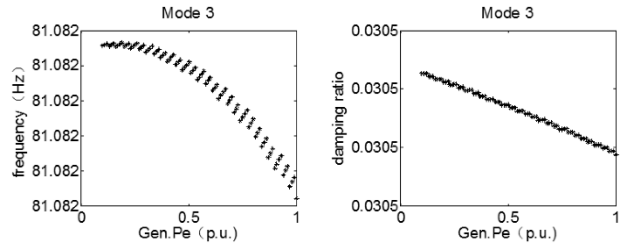

(c) Mode 3

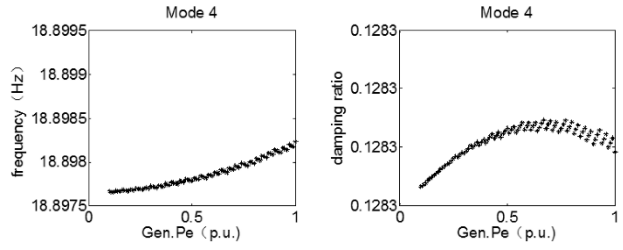

(d) Mode 4

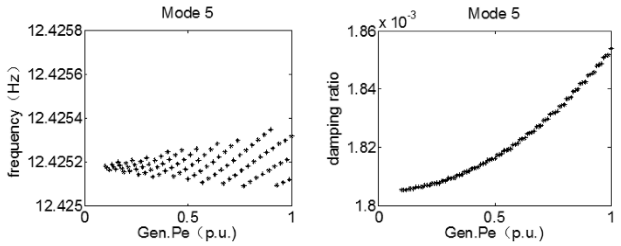

(e) Mode 5

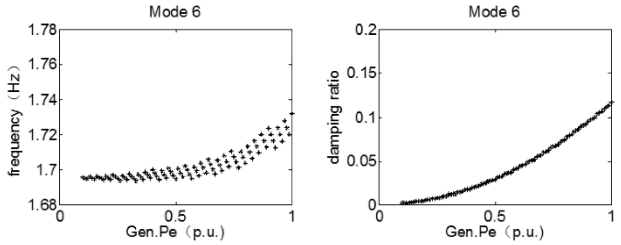

(f) Mode 6

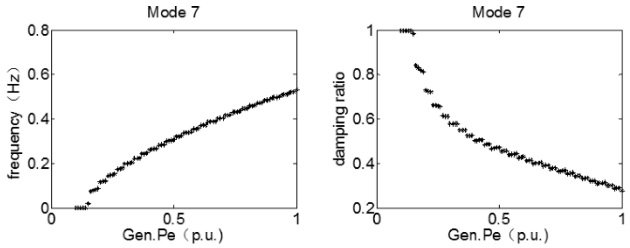

(g) Mode 7

Fig. 5 Variation trend of the oscillation modes for turbine-grid interactions with *Gen.Pe*

Mode 1 and Mode 2 are electrical resonance modes which are caused by generator stator reactance and parallel compensation capacitor. Mode 3 and Mode 4 belong to SSR. Mode 5 and Mode 6 are subject to the sub-synchronous oscillation of turbine shaft. These oscillation modes all have weak association with *Gen.Pe* and change little both in oscillation frequencies and damping ratios.

As *Gen.Pe* increases, Mode 7 keeps increasing its oscillation frequency and decreasing its damping ratio. It is noticeable that Mode 7 does not behave as oscillation mode when *Gen.Pe* is less than 0.14 p.u. It means low-frequency oscillation can be eliminated if generator outputs very little active power. This is a feasible kind of turbine-grid interactions damping design.

5.2. Series capacitor compensation

Series capacitor compensation is a well-known technology and a cost-effective solution to enhance the transient stability and power transmission capacity of the required corridors. However, the series capacitor compensation can produce adverse effects such as SSI with other power system components. A series of simulations are done when the series compensation degree k_{com} changes from 0 to 0.99 by a step of 0.01. k_{com} keeps to be less than 1 because transmission line is an inductive element. Changing regulations for all oscillation modes of turbine-grid interactions with the series compensation can be obtained from Fig.6.

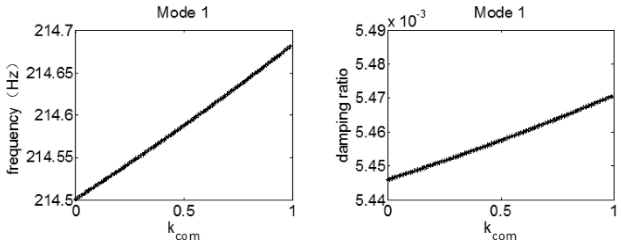

(a) Mode 1

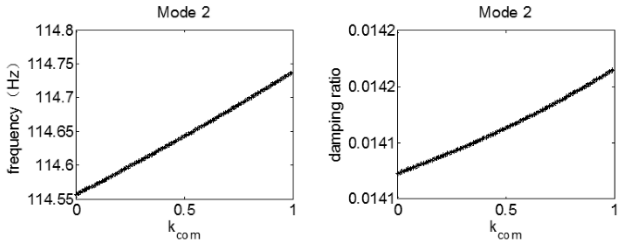

(b) Mode 2

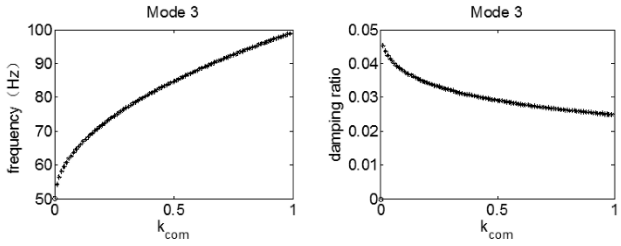

(c) Mode 3

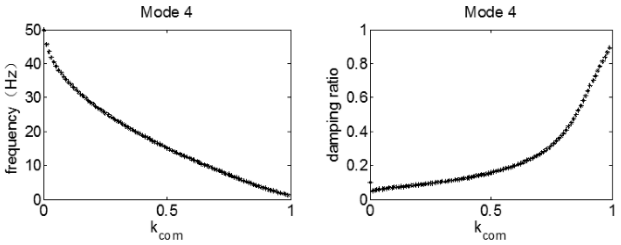

(d) Mode 4

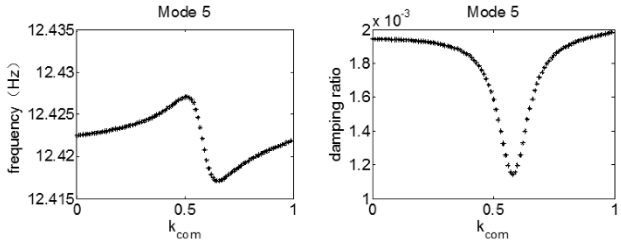

(e) Mode 5

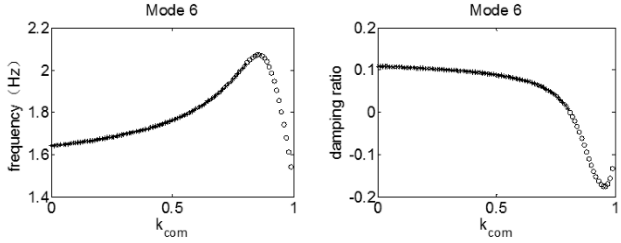

(f) Mode 6

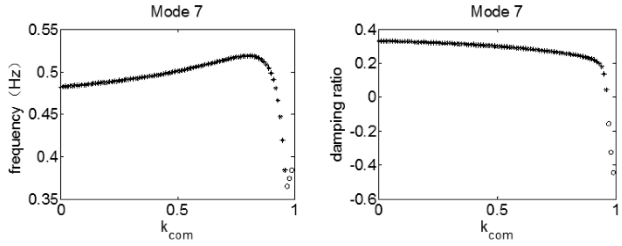

(g) Mode 7

Fig. 6 Variation trend of the oscillation modes for turbine-grid interactions with k_{com}

Mode 1 and Mode 2 can be classified into electrical resonance of generator stator reactance and parallel compensation capacitor. The two oscillation modes both have weak association with k_{com}, resulting little change both in frequencies and damping ratios for the two modes.

Mode 3 and Mode 4 are SSR modes which are caused by the electric resonance of transmission line. The oscillation frequencies $f_s \pm f_e = f_s(1 \pm \sqrt{k_{com}})$ are decided directly by k_{com} so the two modes show opposite variation trends and keep complementary.

Mode 5 and Mode 6 have similar variation trends in damping ratios whereas Mode 5 has little change in frequency and Mode 6's frequency increases at first then decreases. As for damping ratios, they both keep enhancing at first and then weakening. When k_{com} is more than 0.81, Mode 6 becomes unstable. As a result, SSO modes become more and more stable when k_{com} decreases.

Mode 7 is low-frequency oscillation mode. It almost keeps the same characteristics when k_{com} is less than 0.8. When k_{com} becomes larger, the mode increases at first then decreases in frequency and damping ratio keeps weakening all the time.

According to the variation trends of the corresponding oscillation modes, the turbine-grid interactions damping control of those modes can aim at decreasing the series compensation degree k_{com} to some extent.

5.3. Parallel capacitor compensation

Parallel capacitor compensation is used to supply reactive power for generator excitation. The per unit value of $1/x_{PC}$ is equal to the per unit value of the reactive power the parallel capacitor supplies. For example, $1/x_{PC}$ =0.5 means supplying reactive power whose capacity is 50% of system rated capacity. So parallel compensation degree $1/x_{PC}$ changes from 0.01 to 1 by a step of 0.01 when other parameters keep the same. Variation trend of the oscillation modes for turbine-grid interactions with $1/x_{PC}$ is obtained, as shown in Fig.7.

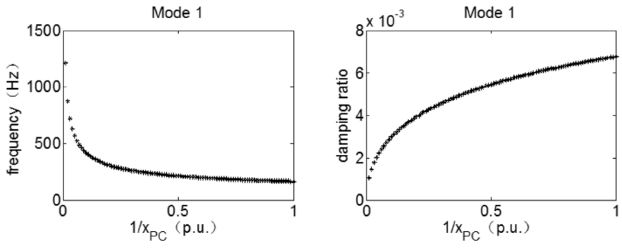

(a) Mode 1

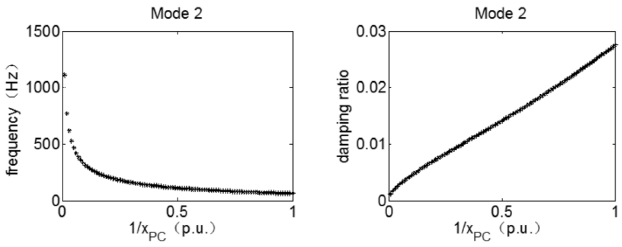

(b) Mode 2

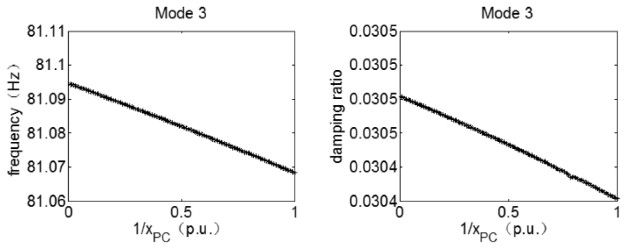

(c) Mode 3

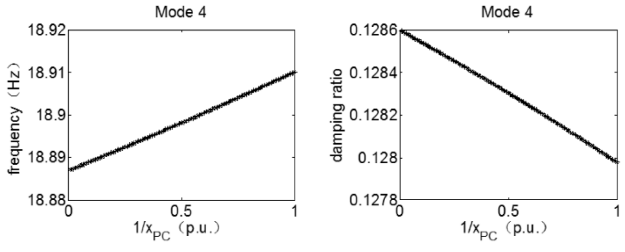

(d) Mode 4

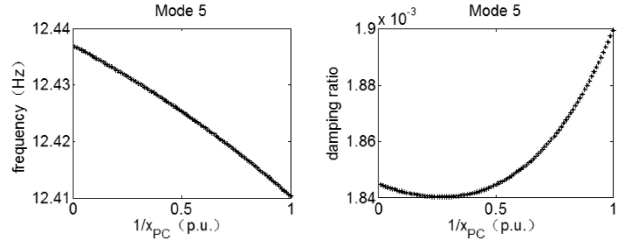

(e) Mode 5

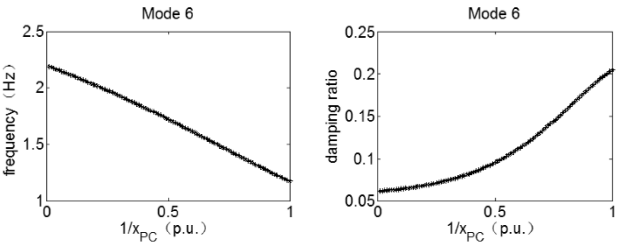

(f) Mode 6

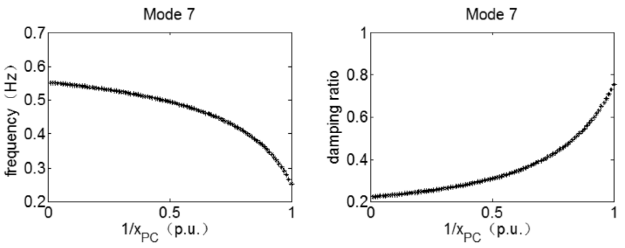

(g) Mode 7

Fig. 7 Variation trend of the oscillation modes for turbine-grid interactions with $1/x_{PC}$

Mode 1 and Mode 2 are electrical resonance modes. As $1/x_{PC}$ increases, the frequencies of two modes decrease obviously. Mode 1's damping ratio keeps becoming weaker and weaker. In Mode 2, damping ratio keeps enhancing all the time.

Mode 3 and Mode 4 belong to SSR, having weak association with $1/x_{PC}$. The two modes changes little both in oscillation frequencies and damping ratios.

Mode 5, Mode 6 and Mode 7 have similar variation trends. As $1/x_{PC}$ increases, the oscillation frequencies of the three modes keep decreasing and the damping ratios keep increasing. Mode 5 and Mode 6 belong to SSO and Mode 7 belongs to low-frequency oscillation.

To sum up, the parallel capacitor compensation has less influence on turbine-grid interactions compared with that of the series capacitor compensation. The damping control design based on it should play a secondary role.

5.4. Verification through Kharitonov polynomials

As shown in the simulations, the system will be unstable in the process of adjusting the series compensation degree of the system from 0 to 1 gradually, especially when the value of k_{com} is greater than 0.81. At the same time, the reasonableness of the simulation results can also be verified through Kharitonov theorem. This part is given in the cases of a series compensation degree equal to 0.4 and 0.82, respectively. The others have the similar approach.

According to the equation (8), the structure of the single FSIG wind generation system is showed as Fig.8 The transfer function of the system is

$$W(s) = C(sI - A)^{-1}B + D \tag{10}$$

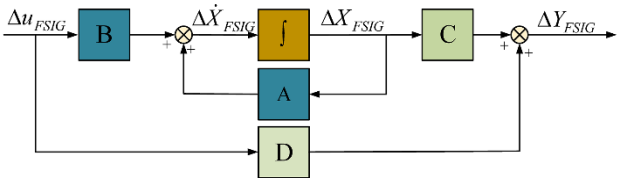

Fig. 8 The structure of the whole system

Therefore, the characteristic polynomial of the system can be expressed as

$$\begin{aligned} P(s) &= |sI - A| \\ &= \sum_{i=0}^{16} c_i s^{16-i} \\ &= c_0 s^{16} + c_1 s^{15} + c_2 s^{14} + \cdots + c_{15} s + c_{16} \end{aligned} \tag{11}$$

It is assumed that with a small disturbance to the value of k_{com}, the coefficients of the characteristic polynomial are bounded as Table 4 and Table 5.

TABLE 4

LOWER AND UPPER LIMITS OF KHARITONOV POLYNOMIAL COEFFICIENTS （K_{COM} =0.4）

i	Lower limit	Upper limit
0	1	1
1	106.331429657046	106.335341624070
2	2621165.25856656	2621361.19597252
3	232526297.340965	232530731.615012
4	1610881882383.56	1611324756104.14
5	106889866802028	106909960996634
6	2.79306605293437e+17	2.79464464330188e+17
7	1.13117642904723e+19	1.13173595505282e+19
8	5.26497652224920e+21	5.27488645497565e+21
9	9.93108367843095e+22	9.93912959597293e+22
10	2.26232658683473e+25	2.26910621873794e+25
11	2.08532174989652e+26	2.09213917479710e+26
12	3.43313696218651e+27	3.44306857494957e+27
13	1.95192874136806e+28	1.95802414274129e+28
14	5.74373340724419e+28	5.76078151573137e+28

15	1.44929540902496e+29	1.45374746839110e+29
16	935062214605838	2.11576066837348e+15

TABLE 5

LOWER AND UPPER LIMITS OF KHARITONOV POLYNOMIAL COEFFICIENTS （K_{COM}=0.82）

i	Lower limit	Upper limit
0	1	1
1	102.972820863848	103.033978008790
2	2703288.07547204	2704067.18959280
3	229661328.727121	229770539.289887
4	1798193829521.29	1799987224458.53
5	112103440903574	112112494068878
6	3.49295544109180e+17	3.49996034009560e+17
7	1.30751062518938e+19	1.30801878729106e+19
8	2.62094462107370e+21	2.63168644027613e+21
9	7.94445857180342e+22	7.95423634219231e+22
10	3.45456466869576e+24	3.54822466812585e+24
11	2.67912867795025e+25	2.75565488510679e+25
12	5.52949364828739e+26	5.68345612111616e+26
13	2.40962085305806e+27	2.49224067502687e+27
14	8.23497103254020e+27	8.49719941648663e+27
15	1.67540903497573e+28	1.74040957074364e+28
16	43651947608134.2	89355884838396.8

As indicated, by applying Kharitonov theorem on the 16th order characteristic equation, the four Kharitonov polynomials can be written as

$$\begin{cases} P_1(s) = c_{0l}s^{16} + c_{1l}s^{15} + c_{2u}s^{14} + \cdots + c_{15u}s + c_{16l} \\ P_2(s) = c_{0l}s^{16} + c_{1u}s^{15} + c_{2u}s^{14} + \cdots + c_{15l}s + c_{16l} \\ P_3(s) = c_{0u}s^{16} + c_{1l}s^{15} + c_{2l}s^{14} + \cdots + c_{15u}s + c_{16u} \\ P_4(s) = c_{0u}s^{16} + c_{1u}s^{15} + c_{2l}s^{14} + \cdots + c_{15l}s + c_{16u} \end{cases} \tag{12}$$

where c_{il} and c_{iu} represent the minimum and maximum bounds of the polynomial coefficients c_i ($i=0,1,2,\cdots,16$).

It can be seen that the different series compensation degree will influence on the stability and dynamic performance of the system. Furthermore, when the series compensation degree equals to 0.4, the corresponding four Kharitonov polynomials are stable by using Hurwitz criterion, whereas two of the four Kharitonov polynomials are unstable when the series compensation degree is 0.82, which are $P_2(s)$ and $P_4(s)$. Obviously, the analysis results are consistent with the simulation results. Adopting the same calculation method above step by step, we can prove that when the series compensation degree is less than 0.81, Kharitonov polynomial criterion shows that the system is stable, otherwise, the system is unstable.

6. CONCLUSIONS

Manifesting as mechanical or electrical oscillation modes, all the interactions between a single FSIG and the grid are studied in this paper, including electrical resonance, SSI and low-frequency oscillation. The paper also studies the influence some variables may have on those interactions. It is found out that the initial operating point, the parallel capacitor compensation and the series capacitor compensation can have either positive or negative impact on the oscillation damping control. The impact depends on the associations between the corresponding interactions and the

variables. For the initial operating point, low-frequency oscillation mode keeps increasing its oscillation frequency and decreasing its damping ratio when the active power output of the generator increases, and other oscillation modes does not change a lot. Low-frequency oscillation can even be eliminated if the generator outputs very little active power. For the series capacitor compensation, SSI and low-frequency oscillation all have obvious changes in frequencies and damping ratios when the series compensation degree increases. Remarkably, SSO and low-frequency oscillation modes becomes unstable when the series compensation degree is more than 0.8. For the parallel capacitor compensation, SSR and low-frequency oscillation modes can be more stable when the reactive power's capacity supplied by the parallel capacitor increases. Nevertheless, it appeared that the parallel capacitor has smaller effects on the damping control than the series capacitor. As a result, both the two kinds of capacitor compensation should be taken into account in turbine-grid interactions damping control design and the control design based on the series capacitor should play a major role. The Kharitonov polynomials provide theoretical proof also.

7. APPENDIX A

TABLE A1

PARAMETERS OF THREE-MASS MODEL

Parameter	Value	p.u.
H_1	$6.41\times10^6\ kg\cdot m^2$	4.50
H_2	$8.79\times10^4\ kg\cdot m^2$	0.12
H_3	$121.5\ kg\cdot m^2$	0.75
K_{12}	$1.455\times10^8\ N\cdot m^2$	0.65
K_{23}	$9.22\times10^4\ N\cdot m^2$	3.62
n	93.75	——

TABLE A2

PARAMETERS OF INDUCTION GENERATOR

Parameter of Motor	Value
n_p	2
X_m	3.9507 p.u.
X_s	0.0924 p.u.
X_r	0.0990 p.u.
R_s	0.0046 p.u.
R_r	0.0055 p.u.

TABLE A3

PARAMETERS OF TRANSMISSION LINES

Parameter of Transmission Lines	Value
X_T	0.044 p.u.
R_T	0.007 p.u.
X_L	8.402 p.u.
R_L	0.8402 p.u.
X_B	0.060 p.u.
R_B	0 p.u.
X_{PC}	2 p.u.
k_{com}	0.4

8. REFERENCES

[1] R. Thresher, M. Robinson, and P. Veers, “To capture the wind,” IEEE Power and Energy Magazine, Vol. 5, No. 6, pp. 34 - 46, Nov.-Dec.2007.

[2] Erlich, and F. Shewarega, “Interaction of large wind power generation plants with the power system,” IEEE International Power and Energy Conference, pp. 12 - 18, Nov. 2006.

[3] Kidd D, Hassink P. Transmission operator perspective of Sub-Synchronous Interaction[C]//Transmission and Distribution Conference and Exposition (T&D), 2012 IEEE PES. IEEE, 2012: 1-3.

[4] S Feng, D Liu, X Yang, X Xiang. The impact of wind power inverse-peaking characteristics on power system low frequency oscillation[C]//Electricity Distribution (CICED), 2012 China International Conference on. IEEE, 2012: 1-4.

[5] Golshannavaz S, Mokhtari M, Nazarpour D. SSR suppression via STATCOM in series compensated wind farm integrations[C]//Electrical Engineering (ICEE), 2011 19th Iranian Conference on. IEEE, 2011: 1-6.

[6] Chen Qiyu, Tim Littler, Han Shushan, Wang Haifeng. Risk assessment model for wind generator tripping off[J]. Proceedings of the CSEE, 2015, 35(3): 576-582.

[7] José Luis Domínguez-Garcíaa, Oriol Gomis-Bellmunt, Fernando D. Bianchia, Andreas Sumper. Power oscillation damping supported by wind power: a review[J]. Renewable and Sustainable Energy Reviews, 2012, 16(7): 4994-5006.

[8] Suriyaarachchi, D. H. R., et al. "A procedure to study sub-synchronous interactions in wind integrated power systems." Power Systems, IEEE Transactions on 28.1 (2013): 377-384.

[9] Wang L, Xie X, Jiang Q, et al. Centralised solution for subsynchronous control interaction of doubly fed induction generators using voltage-sourced converter[J]. IET Generation, Transmission & Distribution, 2015, 9(16): 2751-2759.

[10] Chowdhury M A, Mahmud M A, Shen W, et al. Nonlinear Controller Design for Series-Compensated DFIG-Based Wind Farms to Mitigate Subsynchronous Control Interaction[J]. IEEE Transactions on Energy Conversion, 2017, 32(2): 707-719.

[11] H. A. Mohammadpour and E. Santi, “Sub-synchronous resonance analysis in DFIG-based wind farms: Definitions and problem identification—Part I,” in Proc. IEEE Energy Convers. Congr. Expo., 2014, pp. 812–819.

[12] H. A. Mohammadpour and E. Santi, “SSR damping controller design and optimal placement in rotor-side and grid-side converters of seriescompensated DFIG-based wind farm,” IEEE Trans. Sustain. Energy, vol. 6, no. 2, pp. 388–399, Apr. 2015.

[13] L. Wang, X. Xie, Q. Jiang, H. Liu, Y. Li, and H. Liu, “Investigation of SSR in practical DFIG-based wind farms connected to a series-compensated power system,” IEEE Trans. Power Syst., vol. 30, no. 5, pp. 2772–2779, Sep. 2015.

[14] J. Lv, P. Dong, G. Shi, X. Cai, H. Rao, and J. Chen, “Subsynchronous oscillation of large DFIG-based wind farms integration through MMC-based HVDC,” in Proc. IEEE Int. Conf. Power Syst. Technol. (POWERCON), Oct. 2014, pp. 2401–2408.

[15] H. Liu and J. Sun, “Voltage stability and control of offshore wind farms with AC collection and HVDC transmission,” IEEE J. Emerg. Sel. Topics Power Electron., vol. 2, no. 4, pp. 1181–1189, Dec. 2014.

[16] Xu R, Zhang Y, Lu S, et al. Pulse train-controlled CCM boost converter with suppression of low-frequency oscillation[J]. IET Power Electronics, 2017.

[17] B Lu, Y Li, X Wu, Z Yang. A review of recent advances in wind turbine condition monitoring and fault diagnosis[C]//Power Electronics and Machines in Wind Applications, 2009. PEMWA 2009. IEEE. IEEE, 2009: 1-7.

[18] Habibi F, Naghshbandy A H, Bevrani H. Robust voltage controller design for an isolated Microgrid using Kharitonov’s theorem and D-stability concept[J]. International Journal of Electrical Power & Energy Systems, 2013, 44(1):656-665.

[19] Chowdary N V, Chidambaram M. Robust controller design for First order Plus Time Delay systems using Kharitonov Theorem[J]. IFAC Proceedings Volumes, 2014, 47(1): 184-191.

[20] Qiao X, Luo F, Xu Y. Robust PID controller tuning for uncertain systems based on the constrained Kharitonov's theorem and genetic algorithm[J]. Journal of Computational Information Systems, 2015, 11(9):3195-3202.

[21] Varma R, Moharana A. SSR in double-cage induction generator-based wind farm connected to series-compensated transmission line[J]. Power Systems, IEEE Transactions on, 2013, 28(3): 2573-2583.

[22] Fan L, Yin H, Miao Z. On active/reactive power modulation of DFIG-based wind generation for interarea oscillation damping[J]. Energy Conversion, IEEE Transactions on, 2011, 26(2): 513-521.

[23] Li S, Hao X, Li S. Low-frequency oscillation characteristics of wind power systems with interface including the stator dynamics[C]//Power System Technology (POWERCON), 2010 International Conference on. IEEE, 2010: 1-8.

[24] F Wu, XP Zhang, K Godfrey, P Ju. Small signal stability analysis and optimal control of a wind turbine with doubly fed induction generator[J]. IET Generation, Transmission & Distribution, 2007, 1(5): 751-760.

[25] Y Zhang, D Xie, J Feng, R Wang "Small-signal modeling and modal analysis of wind turbine based on three-mass shaft model." Electric Power Components and Systems 42.7 (2014): 693-702.

[26] Kundur P (1994) Power system stability and control. McGraw Hill, New York, NY, USA

9. ACKNOWLEDGMENT

This work was supported by the National Natural Science Foundation of China (51677114 and 51277119) and Research Program of State Grid Corporation of China (SGTYHT/16-JS-198).

10. AUTHOR BIOGRAPHIES

Da Xie received his B.S. from SJTU, Shanghai, China, in 1991; his M.S. from HIT, Harbin, China, in 1996; and his Ph.D. from SJTU in 1999. His research focuses on power transmission and distribution of smart grids, micro-grid management, and grid-connected techniques of renewable energy. Corresponding Author E-mail: profxzg@hotmail.com.

Wangping Wu received the B.S degree from Harbin Engineering University, Harbin, China, in 2015. Now, he is a postgraduate majoring in electrical engineering in Shanghai Jiao Tong University, Shanghai, China. His current research interests are wind power modeling, renewable energy and power system analysis. E-mail:wode15sjtu@sjtu.edu.cn.

Xitian Wang received the B.E. and Ph.D. from Harbin Institute of Technology, Harbin, China, in 1995 and 2001, respectively. Currently, he is an Associate Professor in the Department of Electrical Engineering, Shanghai Jiao Tong University, China. His research interests include dynamics, simulation, and control of electromechanical interactions in power systems. E-mail: x.t.wang@sjtu.edu.cn.

Chenghong Gu received the B.S and M.S. from Shanghai University of Electric Power and SJTU, Shanghai, China, in 2003 and 2007, respectively, and the Ph.D. from the University of Bath, U.K., in 2010. Now, he is a KTA fellow in the Department of Electronic and Electrical Engineering, University of Bath. His research interests are power system planning and smart grid. E-mail: c.gu@bath.ac.uk.

Yanchi Zhang received his Ph.D. in the Department of Automation, East China University of Science and Technology, Shanghai, China. Currently, he is an Associate Professor in the Department of Electrical Engineering, Shanghai Dian Ji University. His main research interests are wind power technology and flexible AC transmission systems (FACTS). E-mail: zhangyc@sdju.edu.cn.

Furong Li received the B.Eng. degree in electrical engineering from Hohai University, Nanjing, China, in 1990, and the Ph.D. degree in electrical engineering from Liverpool John Moores University, Liverpool, U.K., in 1997. She is a Professor in the Power and Energy Systems Group, University of Bath, Bath, U.K. Her current research interests include power system planning, operation, automation, and power system economics. E-mail: f.li@bath.ac.uk.